

Modular multi-input converter design for hybrid energy storage system used in traction power substation

Chuen Ling Toh^{1,2}, Ching Sin Tan², Chee Wei Tan³

¹Department of Electrical and Electronic Engineering, Universiti Tenaga Nasional, Selangor, Malaysia

²Institute of Power Engineering, Universiti Tenaga Nasional, Selangor, Malaysia

³Department of Electrical Power Engineering, Faculty of Electrical Engineering, Universiti Teknologi Malaysia, Johor Bahru, Malaysia

Article Info

Article history:

Received Jul 29, 2024

Revised Nov 7, 2024

Accepted Nov 28, 2024

Keywords:

Battery
DC railway power substation
Hybrid energy storage system
Modular multi-input converter
Supercapacitor

ABSTRACT

Hybrid energy storage system (HESS) which consists of battery and supercapacitor is proposed to store bulk regenerative braking energy for future traction power substation. This system aims to optimize energy utilization and enhance the sustainability of rail transport. To facilitate bidirectional power flow between the traction network and the HESS, this paper introduces a modular multi-input converter (MMIC) to dynamically transfers during both braking and acceleration phases of train operation. The proposed MMIC operates in multiple modes, allowing for seamless energy exchange between the battery and supercapacitor, thus minimizing the depth of discharge of the battery and extending its lifespan. A comprehensive theoretical analysis of the MMIC is presented, detailing its four distinct operating modes. Additionally, simulation model of a 1.5 kV traction power substation with 500 kWh HESS is developed to validate the performance of the MMIC during steady-state operation. The findings demonstrate significant improvements in energy recovery and storage capabilities, underscoring the potential of the HESS to support future traction power substations in achieving higher efficiency and sustainability.

This is an open access article under the [CC BY-SA](https://creativecommons.org/licenses/by-sa/4.0/) license.



Corresponding Author:

Chuen Ling Toh
Institute of Power Engineering, Universiti Tenaga Nasional
St. Ikram-Uniten, 43000 Kajang, Selangor, Malaysia
Email: chuenling@uniten.edu.my

1. INTRODUCTION

DC electrified railway system used to integrate multi-pulse diode rectifier transformer system to power up the railway networks. The multi-pulse diode rectifier transformer system offers low distortion to the utility grid [1]. However, it also blocks the returning of the braking energy produced by a stopping train to the grid. In order to properly dissipated the excessive braking energy, a set of resistor bank are commonly installed. As a result, the regenerative braking is dissipated as heat at a substation. With the aim to achieve sustainable development goal, some railway companies have proposed and integrated energy storage system onboard of the train vehicle [2], [3] as well as in a traction power substation (TPS) [4], [5]. Figure 1 shows the block diagram of the braking energy flows back to onboard energy storage system (OESS) and wayside energy storage system (WESS).

The OESS used to mount the battery banks and the DC-DC converter on the train vehicle. Therefore, the mass and volume become the major constraint of the total capacity of OESS. Some literatures had summarized that WESS is more practical in term of cost effectiveness for energy saving [6]. The WESS can be easily integrated to the existing TPS, where the energy storage system may just be configured in parallel to the existing resistor bank as shown in Figure 1. The WESS will serve as voltage compensator and a secondary traction power supply to accelerate trains form leaving a passenger station. A field test result had shown that a

TPS with WESS may save energy consumption in the range of 15% – 30% (approximate of 700 kWh/day) [4]. WESS may also act as backup power supply to continue moving a train to the nearest passenger station during power outages. In general, WESS consists of three major components, namely energy storage elements, power converter and controllers. Supercapacitors (SC) and electrochemical batteries are two popular choices of energy storage used in WESS [7], [8]. These energy storages offer rapid charging performance to store large amount of regenerative power in short duration.

Supercapacitor-based WESS was first been proposed as voltage compensator due to a typical 50% DC voltage drop is measured at final train station. A high-capacity and high-volume SC bank is designed to solve the issue using a conventional buck-boost converter [9]. SC capacity and positioning optimization are two major research areas for SC-based WESS [10], [11]. On the other hand, battery-based WESS has been widely proposed as well. Battery technology such as SCiB [4] and Lithium-ion [12] are employed in some pilot projects at TPS. Bidirectional DC-DC converter is the key converter to charge and discharge the battery bank. Interleaved bidirectional DC-DC converter [13], [14] is one of the conventional topologies widely used in battery-based WESS. Some recent research works had also proposed zero-current switching bidirectional DC-DC converter [15], and series compensation with four-quadrant chopper in battery-based WESS applications [4]. Figure 2 shows the bidirectional DC-DC converter circuit configuration used in SC-based and battery-based WESS.

Since supercapacitor have higher durability with faster response time while battery offers high energy and power densities, combination of these two energy storages in a WESS may be another potential solution for future TPS. This hybrid configuration had been widely adopted in electric car energy storage system using multi-input bidirectional DC-DC converter [16]-[26]. Thus, this paper presents an analysis of implementing a modular multiple-input bidirectional DC-DC power converter [17] for future TPS. The circuit topology and the operating principal of the proposed converter will be presented in section 2. Section 3 presents the simulation analysis of the converter and a conclusion will be summarized in section 4.

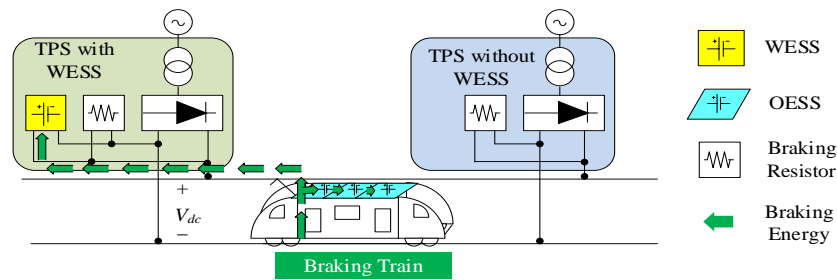


Figure 1. Regenerative braking energy flows back to onboard energy storage system (OESS) and wayside energy storage system (WESS) at a traction power substation (TPS)

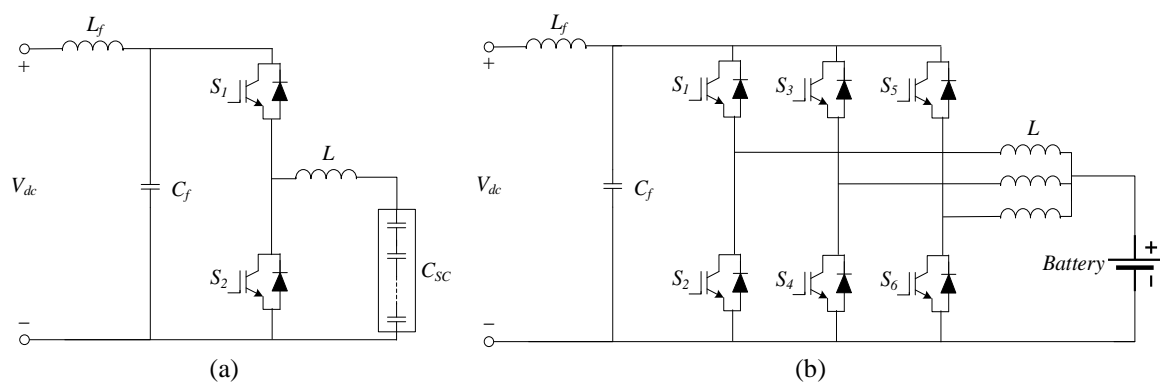


Figure 2. Bidirectional DC-DC converter circuit proposed in WESS: (a) SC- based [9] and (b) battery-based [13]

2. MULTI-INPUT CONVERTER CIRCUIT OPERATION AND ANALYSIS

The hybrid energy storage system (HESS) proposed for TPS consists of battery and supercapacitor. A bidirectional DC-DC converter can be implemented to enable power transferred between these energy storage elements and the DC-link of the traction power substation. When the railway vehicle is braking,

excessive regenerative power can be stored into the HESS. Consequently, this power can be delivered back to the DC-link when the railway vehicle is accelerating. Figure 3 presents the circuit of the modular multi-input converter (MMIC). Three set of half-bridge power modules are used to form the MMIC, namely P_1 , P_2 , and P_3 . Each power module is configured with a series connected power switches, S_{ui} (upper switch) and S_{li} (lower switch). The battery, supercapacitor and the DC-link network terminal are connected parallel to each of the half bridge power module. Inductor L_1 and L_2 are used to interconnect the energy storage elements to the DC-link as shown in Figure 3. This modular design gives full flexibility for future energy storage expansion. The power can be transferred between the DC-link and the HESS by controlling the conduction of appropriate power switches. Table 1 show the main operation modes of the MMIC with switching duty ratio for each power switch. In general, operating mode A aims to store the regenerative braking energy to the HESS, while mode B enables the energy transfer from HESS to accelerate a departing train. Operating mode C and D are designed to improve the battery lifespan. The details of each operating mode will be further elaborated in the following sub-sections. All power semiconductors are assumed ideal and identical inductances are employed.

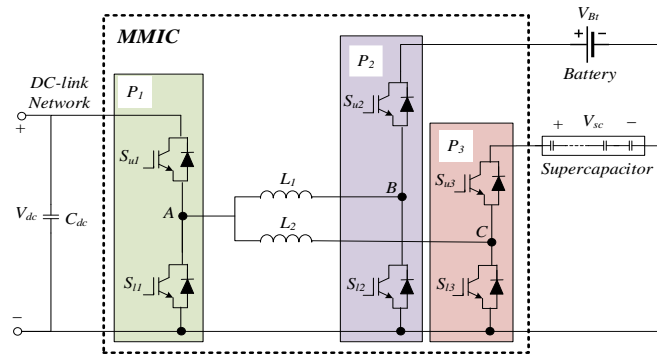


Figure 3. Modular multi-input converter (MMIC) circuit

Table 1. Switching duty cycle of power switches for different operating modes

Mode	Operation	S_{u1}	S_{l1}	S_{u2}	S_{l2}	S_{u3}	S_{l3}
A	DC-link charges the battery and supercapacitor	D_{A1}	$1 - D_{A1}$	D_{A2}	$1 - D_{A2}$	1	0
B	Battery and supercapacitor drive the DC-link	$1 - D_{B1}$	D_{B1}	D_{B2}	$1 - D_{B2}$	D_{B3}	$1 - D_{B3}$
C	Battery drives the supercapacitor	0	0	1	0	$1 - D_C$	D_C
D	Supercapacitor drives the battery	0	0	1	0	D_D	$1 - D_D$

2.1. Power transfer from DC-link to both energy storage elements

The DC-link voltage, V_{dc} , is defined as input source to the MMIC in operating mode A. The converter is controlled to charge the battery and supercapacitor. It is expected that the braking power of a train can be much higher than the battery storage can absorb, therefore the supercapacitor is proposed for TPS to capture as much as the regenerative power. Figure 4 shows the equivalent circuit of the converter for three different switching intervals. Figure 5 illustrates the voltage and current waveforms of inductors L_1 and L_2 aligned with the switching events for all the operating modes. By referring to Figure 5(a), it is highlighted that the upper and lower power switches in each power module must be controlled complementary in operating mode A as listed in Table 1.

Under steady-state operation, all energy storage elements (inductors, battery, and supercapacitor) are receiving charged from the DC-link network during T_1 interval. The charging events are shown with a positive slope of inductors current, i_{L1} and i_{L2} being depicted. Power switch S_{u1} is triggered off during T_2 interval, as a result inductors L_1 and L_2 start to release their storage energies to battery and supercapacitor respectively. Lastly by turning off power switch S_{u2} during T_3 interval, the battery is stop charging with inductor current i_{L1} remains at its minimum current level until next switching cycle is initiated. However, the supercapacitor continuous received charged from L_2 throughout T_3 interval. To simplify the analysis, the ripple inductor currents of L_1 and L_2 is derived in term of its positive, Δi_{L1}^+ , Δi_{L2}^+ , and negative slopes Δi_{L1}^- , Δi_{L2}^- , as (1) and (2).

$$\Delta i_{L1}^+ = \frac{(V_{dc} - V_{Bt})}{L_1} D_{A1} T_{sw} ; \quad \Delta i_{L1}^- = \frac{(-V_{Bt})}{L_1} (D_{A2} - D_{A1}) T_{sw} \quad (1)$$

$$\Delta i_{L2}^+ = \frac{(V_{dc} - V_{SC})}{L_2} D_{A1} T_{sw} ; \quad \Delta i_{L2}^- = \frac{(-V_{SC})}{L_2} (1 - D_{A1}) T_{sw} \quad (2)$$

By assuming the net change in each inductor current over one period is zero, i.e. (3) and (4).

$$\Delta i_{L1}^+ + \Delta i_{L1}^- = 0 \quad (3)$$

$$\Delta i_{L2}^+ + \Delta i_{L2}^- = 0 \quad (4)$$

The relation between DC-link voltage, V_{dc} , battery voltage, V_{Bt} , and supercapacitor voltage, V_{sc} , can be generally formularized as (5) and (6).

$$V_{Bt} = \left(\frac{D_{A1}}{D_{A2}} \right) V_{dc} \quad (5)$$

$$V_{sc} = D_{A1} V_{dc} \quad (6)$$

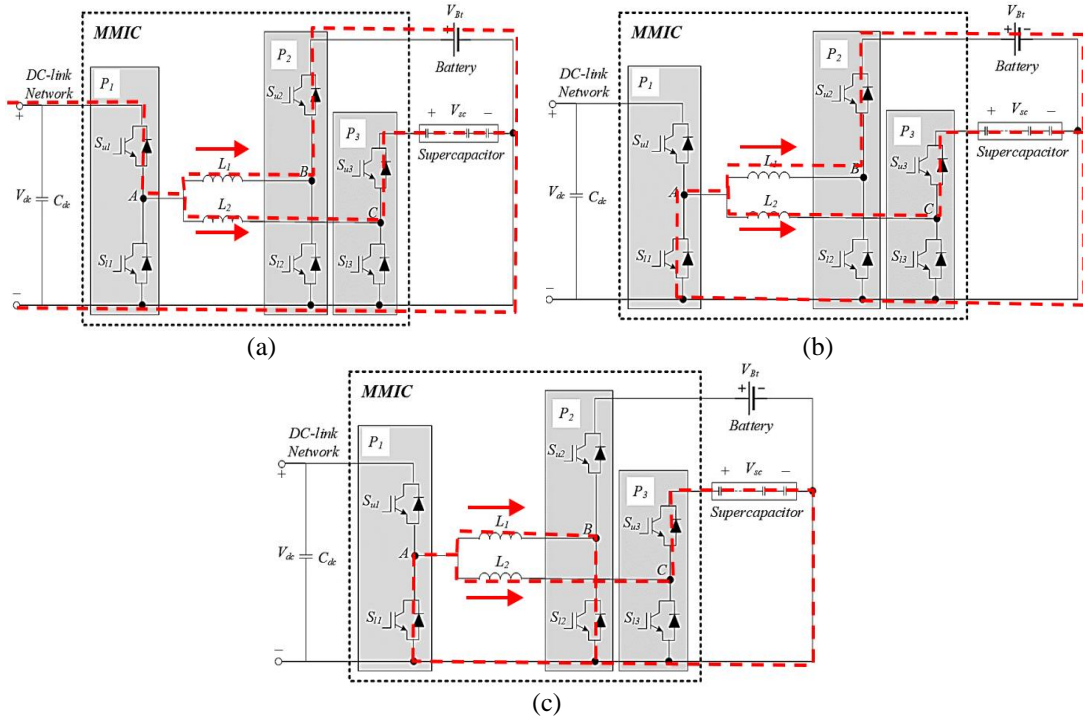


Figure 4. Equivalent circuit of operating modes A for different switching interval: (a) T_1 , (b) T_2 , and (c) T_3

2.2. Power transfer from both energy storage elements to DC-link

In order to accelerate a train from a passenger station, the utility grid needs to supply excessive power to the TPS. If a TPS is equipped with HESS, both the battery and supercapacitor energies can be injected to the DC-link network (operating mode B). The switching states of this operating mode is illustrated in Figure 5(b) with its equivalent circuits presented in Figure 6. Both inductors L_1 and L_2 are being charged by the battery and supercapacitor during T_1 interval as shown in Figure 6(a). Inductor currents are increasing gradually. As power switch S_{u2} is triggered off in T_2 interval (Figure 6(b)), the inductor L_1 holds its current at its maximum current level. Whereas, inductor L_2 is being charged continuously throughout T_2 interval. The supercapacitor is stopped from delivering its energy when S_{u3} is triggered off in T_3 interval as shown in Figure 6(c). Both inductors will release their pre-storage charges to the DC-link terminal during T_3 interval. The relation between DC-link voltage, V_{dc} , battery voltage, V_{Bt} , and supercapacitor voltage, V_{sc} , can be generally formularized as follows using the same approach presented in section 2.1 (the net change in each inductor current over one period is zero).

$$V_{dc} = \left(\frac{D_{B2}}{1-D_{B1}} \right) V_{Bt} \quad (7)$$

$$V_{dc} = \left(\frac{D_{B1}}{1-D_{B1}} \right) V_{sc} \quad (8)$$

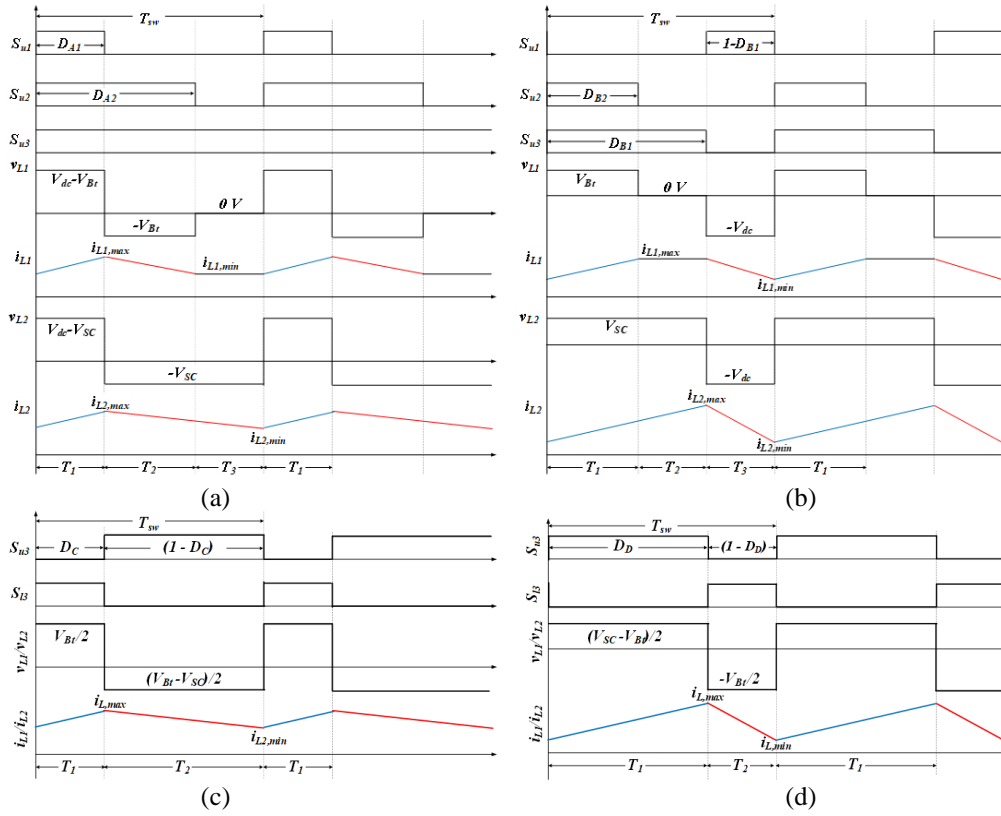
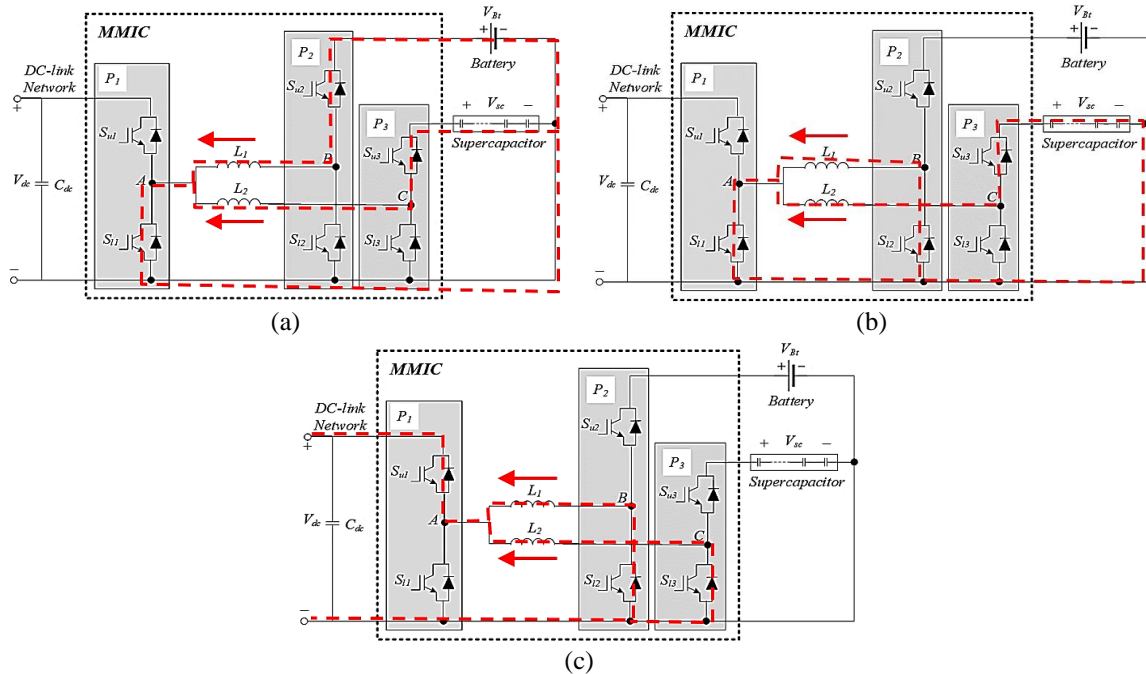


Figure 5. Steady-state waveforms analysis of operating modes: (a) A, (b) B, (c) C, and (d) D

Figure 6. Equivalent circuit of operating modes B for different switching interval: (a) T_1 , (b) T_2 , and (c) T_3

2.3. Power transfer from battery to supercapacitor

Operating mode C mainly aims to discharge the battery energy to the supercapacitor. As listed in Table 1, the power module, P_3 , will be switched accordingly with a duty ratio, D_c , throughout this operation mode. It is highlighted that S_{u1} , S_{l1} , and S_{l2} , are permanently powering off, whereas S_{u2} will constantly be turned on. Figures

7(a) and 7(b) clearly indicate the current paths of this operating mode. By turning on S_{i3} , during T_1 interval, the battery charges the identical inductances L_1 and L_2 . Referring to Figure 5(c), the battery voltage is divided in half by the inductances resulting with the slope of the battery discharging current also being more lenient. When the upper switch, S_{u3} , is switching on during T_2 interval, the supercapacitor receives charge from battery as well as the inductances. By assuming the net change in each inductor current over one period is zero, the relation between V_{sc} and V_{Bt} can be expressed as (9). The (9) clearly shows that the MMIC is operating in boosting mode.

$$V_{sc} = \left(\frac{1}{1-D_c} \right) V_{Bt} \quad (9)$$

2.4. Power transfer from supercapacitor to battery

The MMIC is controlled as a buck converter to charge the battery with the supercapacitor in operating mode D. Power modules P_1 and P_2 are set similarly to operating mode C while power module, P_3 , will be switched accordingly with a duty ratio, D_D , as shown in Figures 7(c) and 7(d). The supercapacitor releases its charges to inductances and battery by switching on S_{u3} throughout T_1 interval. The supercapacitor is disconnected when the lower switch, S_{i3} , is triggered on. The inductance current is freewheeling through the circuit in T_2 interval showing a negative current slope as presented in Figure 5(d). By assuming the net change in each inductor current over one period is zero, the relation between V_{sc} and V_{Bt} can be expressed as (10).

$$V_{Bt} = D_D V_{sc} \quad (10)$$

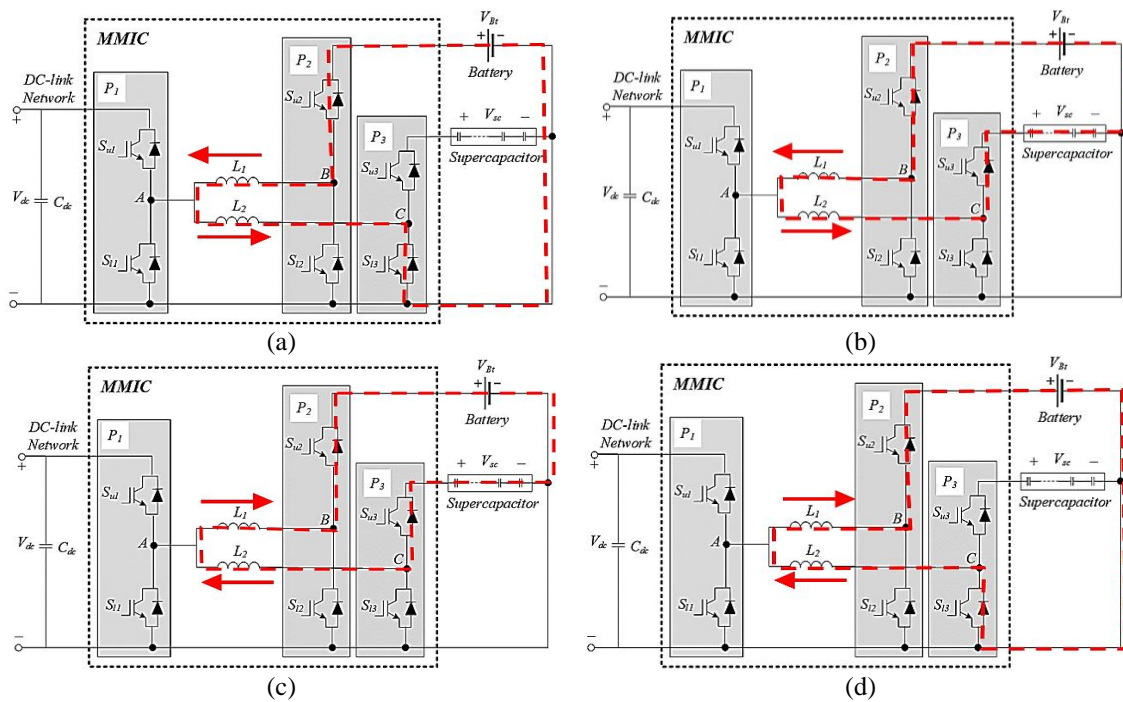


Figure 7. Equivalent circuit of operating modes C and D: (a) mode C switching interval T_1 , (b) mode C switching interval T_2 , (c) mode D switching interval T_1 , and (d) mode D switching interval T_2

3. SIMULATION AND ANALYSIS

In order to analyze the operation modes of MMIC for a future TPS, a simulation model as shown in Figure 8 is developed using MATLAB/Simulink. The operation of a train vehicle is modelled by the Traction Mode control block. By setting the traction mode control block with logic '1', the RL -load will be connected to the DC-link terminal showing a motoring train consuming electrical power. Likewise, if regenerative braking energy is supplying to the DC-link terminal, the DC-voltage source will be enabled, (Traction Mode = 0). The hybrid energy storage elements (battery and supercapacitor) proposed in this simulation work, are assumed to support a total energy requirement of 500 kWh. Assume that, 50 kWh of energy will be stored in supercapacitor while the remaining energy will be stored by the battery for longer-duration power supply. Table 2 summarizes the HESS simulation parameters. The MMIC proposed in this simulation is assumed rated at 6 MVA, 1500 V

mainly to handle the peak power demands and short bursts of energy to and from the supercapacitor. The switching frequency is set to 5 kHz. This paper only focuses on the steady-state analysis of the MMIC operation.

Figures 9(a) and 9(b) show the simulation results when the regenerative power (traction mode = 0) is transmitted to charge the battery and supercapacitor respectively. To further analyze the steady state operation of MMIC in mode A, the duty cycles of power switches S_1 , S_3 , and S_5 are set as 45%, 65%, and 100% accordingly with both the initial state-of-charge (SoC) for both battery and supercapacitor are set to 40%. As shown in Figure 9(a) when power switches S_1 and S_3 are turned on simultaneously, the battery is charged to a peak current of 600 A. By turning off S_1 , the battery current is then circulating through the battery and inductance L_1 for about 20% of the switching interval. The battery is then disconnected from L_1 by triggering off S_3 for the last 35% of the switching interval. This switching scheme manages to regulate the charging current at an average of about 400 A. On the other hand, the supercapacitor is fully connected to the DC link throughout mode A. As S_5 is being turned on continuously, power switch S_1 becomes the dominant switch to control the supercapacitor charging current. Figure 9(b) clearly shows the MMIC is operated in buck conversion mode between the DC-link and supercapacitor. By switching on S_1 , the supercapacitor is charged to a peak current of 2160 A. When S_1 is triggered off at the end of the switching cycle, the charging current reduces to 2070 A.

The hybrid energy storage may act as a secondary supply to minimize the utilization of grid power when a train is accelerating (traction mode = 1). Figures 9(c) and 9(d) present the steady-state simulation results of the HESS discharging events via the control of MMIC. Assuming that the initial SoC for both hybrid storage elements is 96%. Power switches S_3 , and S_5 are controlled with a duty cycle of 35% and 55%. Power switch S_1 must be toggled complementarily to S_5 throughout operating mode B. The energy inside the battery and supercapacitors are transferred to inductances, L_1 , and L_2 by turning on switches S_3 , and S_5 . When power switch S_1 is turned on, the DC-link will receive energy supply from L_1 , and L_2 . The peak discharging current of the battery and supercapacitor are recorded at 780 A and 2.5 kA approximately.

In order to validate the energy transfer between the battery and supercapacitor, power switches S_1 , S_2 , and S_4 should be permanently turned-off, while S_3 must always triggered on. In operating mode C, the initial SoC of the battery and supercapacitor are set to 96% and 40% as shown in Figures 10(a) and 10(b). Power switches S_5 and S_6 are triggered complementarily with a duty cycle of 45%, the methodology is to boost up the battery voltage in order to charge the supercapacitor. Peak discharging current of the battery may reach 715 A. Conversely, in order to reverse the power flow, Power switches S_5 and S_6 are controlled to step down supercapacitor voltage in order to charge the battery. Figures 10(c) and 10(d) show the simulation results of mode D operation with a duty cycle set to 70%. The initial state of battery is assumed as 40% while the supercapacitor is set to 96%. The battery charging current is controlled with an average of 386 A with a ripple current of 28 A. This is mainly due to the filtering effect of identical inductances, L_1 and L_2 .

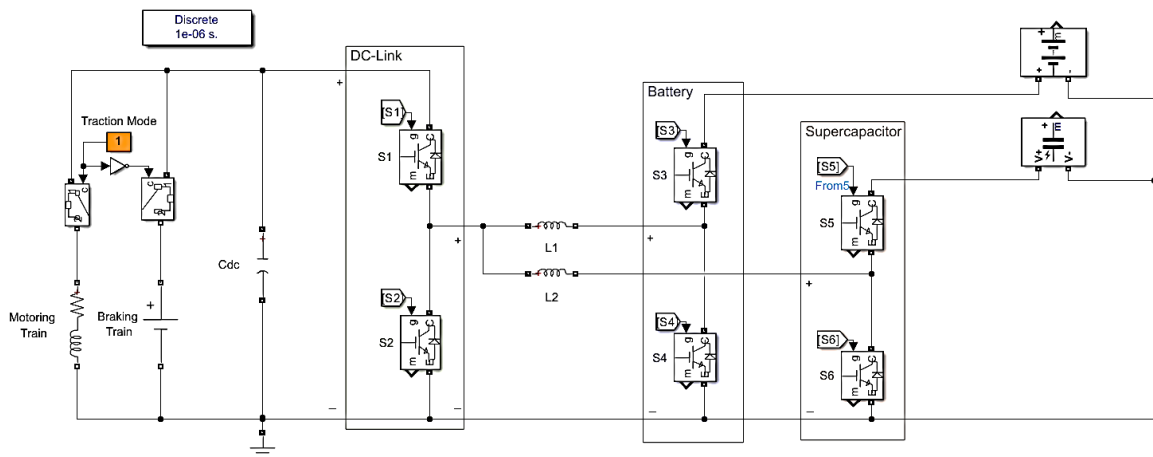


Figure 8. Simulation model of the modular multi-input converter (MMIC)

Table 2. Simulation parameters of the HESS in a DC traction power substation

Train operation modelling [26]		Lithium-ion battery module, 100Ah, 3.6 V		Supercapacitor Maxwell BCAP3000, 2.7 V	
Braking Train, V_{dc}	1850 V	Nominal voltage	1500 V	Total nominal voltage	1500 V
Motoring Train, R	0.2 Ω	C-rated per-string	4C	Total capacitance	160 F
Motoring Train, L	0.75 mH	Number of series-connected modules	417	Number of series-connected cells	556
DC-link	1 mF	Number of parallel strings	3	Number of parallel strings	30
Capacitance, C_{dc}		Inductor, L_1	1 mH	Inductor, L_2	1 mH

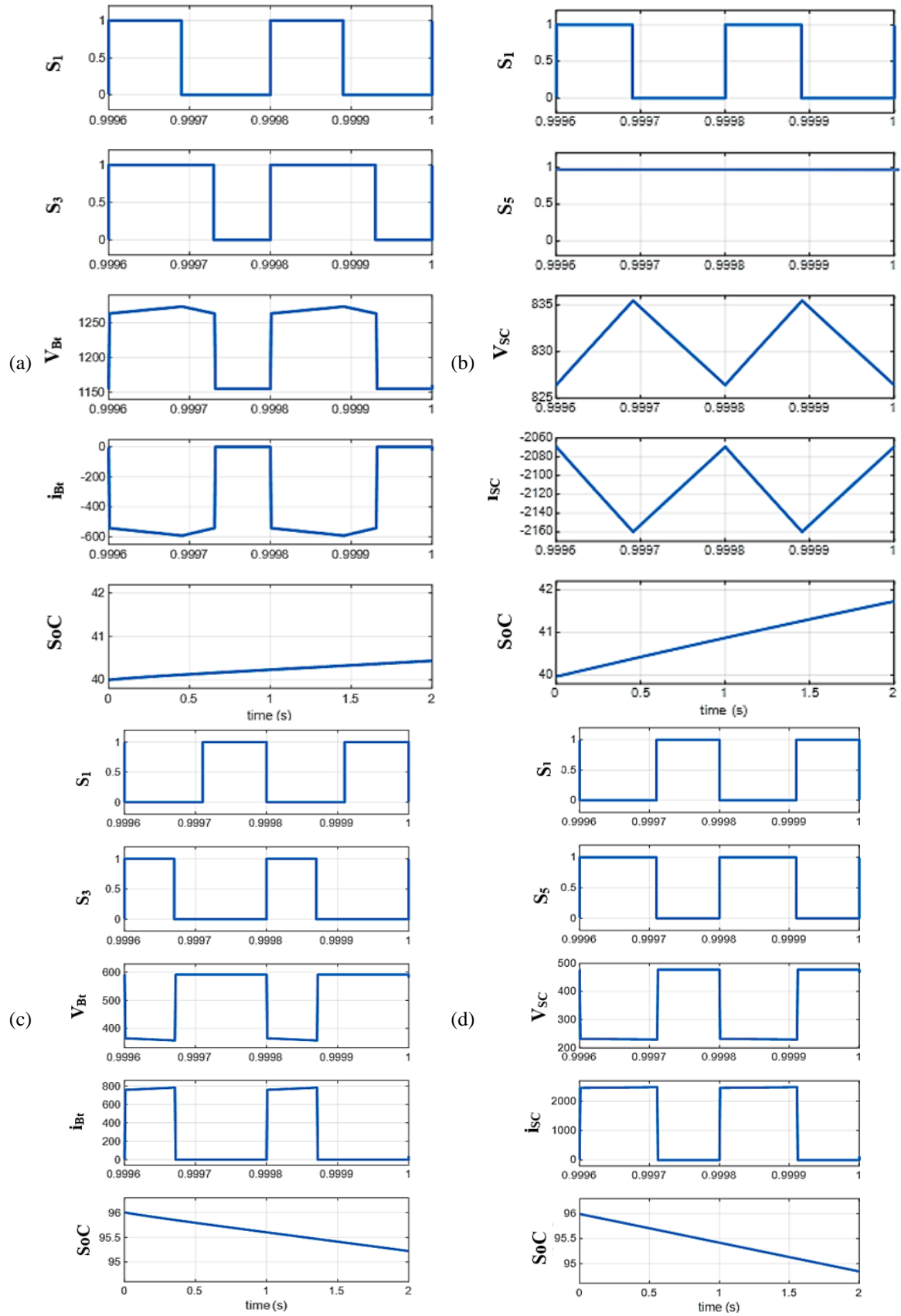


Figure 9. Simulation results for (a) battery charging in mode A, (b) supercapacitor charging in mode A, (c) battery discharging in mode B, and (d) supercapacitor discharging in mode B

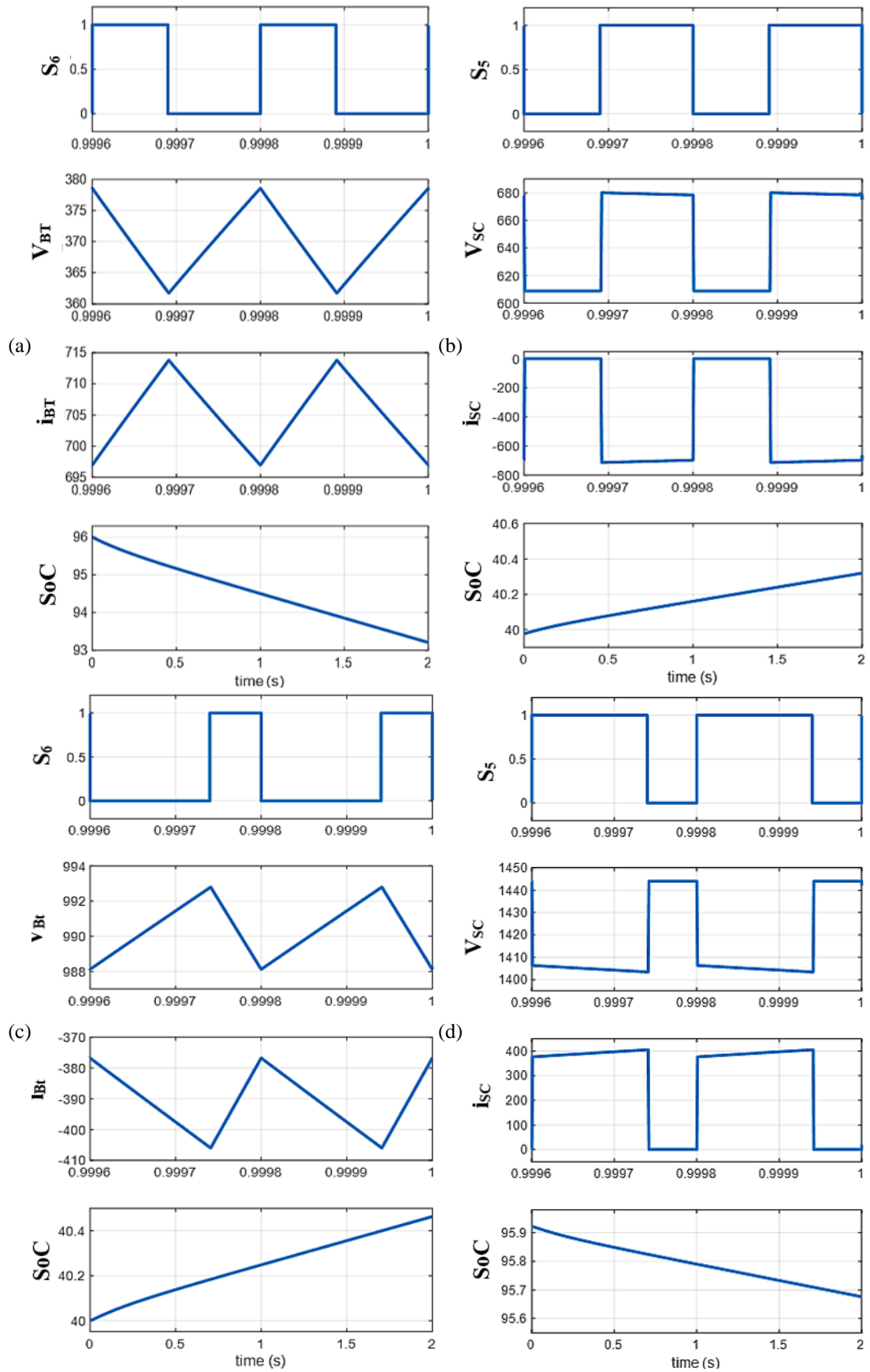


Figure 10. Simulation results for (a) battery discharging in mode C, (b) supercapacitor charging in mode C, (c) battery charging in mode D, and (d) supercapacitor discharging in mode D

4. CONCLUSION

Some traction power substations had been retrofitted with battery-based wayside energy storage system (WESS). However, depends on the capacity of the WESS, some braking power may still be dissipated. Thus, this paper presents a study of integrating hybrid energy storage system (HESS) for future traction power substation. The proposed HESS consists of battery and supercapacitor to capture the bulk regenerative power. A modular multi-input converter (MMIC) which enables bidirectional power flow between the traction DC-link, battery and supercapacitor is modelled and simulated for steady-state analysis. The MMIC can be controlled in boost and buck conversion to cater for different voltage level of supplies. The circuit analysis of the MMIC for four operation modes had been presented and validated through simulation. The simulation results prove that supercapacitor can quickly capture and store the energy generated by a braking train in mode A. During the acceleration of a train, the supercapacitor prevents the deep discharges and high current spikes of a battery in mode B. Lastly in mode C and D, the MMIC can be controlled to reduce depth of discharge for the battery by providing a buffer for energy demands with the help of supercapacitor.

ACKNOWLEDGEMENTS

The authors are pleased to express their appreciation to the Universiti Tenaga Nasional for sponsoring the BOLD Refresh 2025 to conduct this research. Project code: J510050956.




REFERENCES

- [1] S. A. Assefa and A. B. Kebede, "Harmonic analysis of traction power supply system: case study of Addis Ababa light rail transit," *IET Electrical Systems in Transportation*, no. May, 2021, doi: 10.1049/els2.12019.
- [2] G. A. M. Nasution, M. Matsumoto, and M. Hagiwara, "Bidirectional Chopper With Single-Cell Auxiliary Full-Bridge Converter for Onboard Battery Energy Storage System," *IEEE Transactions on Power Electronics*, vol. 39, no. 8, pp. 10021–10033, 2024, doi: 10.1109/TPEL.2024.3392923.
- [3] R. Mao, J. Mi, Y. Shao, Z. Yang, X. Ma, and S. Yang, "Coordinated Energy Management Strategy of Onboard Energy Storage System in Urban Rail Transit," in *2023 IEEE 6th International Electrical and Energy Conference, CIEEC 2023*, 2023, pp. 2649–2654, doi: 10.1109/CIEEC58067.2023.10165857.
- [4] N. Satake *et al.*, "Traction Energy Storage Systems applied with SCiB™," in *2022 International Power Electronics Conference (IPEC-Himeji 2022- ECCE Asia)*, IEEE, May 2022, pp. 1113–1119, doi: 10.23919/IPEC-Himeji2022-ECCE53331.2022.9806922.
- [5] R. F. P. Paternost *et al.*, "Energy Storage Management in Support of Trolleybus Traction Power Systems," in *2022 International Symposium on Power Electronics, Electrical Drives, Automation and Motion, SPEEDAM 2022*, 2022, pp. 252–257, doi: 10.1109/SPEEDAM53979.2022.9842162.
- [6] A. Di Pasquale, E. Fedele, D. Iannuzzi, and M. Pagano, "Contribution of Wayside Energy Storage Systems to Short Circuit Currents in DC Railway Traction Power Systems," in *2022 International Power Electronics Conference, IPEC-Himeji 2022-ECCE Asia*, 2022, pp. 1101–1106, doi: 10.23919/IPEC-Himeji2022-ECCE53331.2022.9807030.
- [7] A. D. Femine, D. Gallo, C. Landi, and M. Luiso, "Energy Recovering from Regenerative Braking in DC Railway System," in *2023 International Conference on Clean Electrical Power, ICCEP 2023*, 2023, pp. 818–823, doi: 10.1109/ICCEP57914.2023.10247479.
- [8] G. Graber, V. Calderaro, V. Galdi, L. Ippolito, and G. Massa, "Impact Assessment of Energy Storage Systems Supporting DC Railways on AC Power Grids," *IEEE Access*, vol. 10, pp. 10783–10798, 2022, doi: 10.1109/ACCESS.2022.3145239.
- [9] A. Rufer, D. Hotellier, and P. Barrade, "A supercapacitor-based energy-storage substation for voltage-compensation in weak transportation networks," 2003, doi: 10.1109/PTC.2003.1304470.
- [10] T. Ratniyomchai, S. Hillmansen, and P. Tricoli, "Optimal capacity and positioning of stationary supercapacitors for light rail vehicle systems," in *2014 International Symposium on Power Electronics, Electrical Drives, Automation and Motion, SPEEDAM 2014*, 2014, pp. 807–812, doi: 10.1109/SPEEDAM.2014.6872019.
- [11] V. Calderaro, V. Galdi, G. Graber, and A. Piccolo, "Optimal siting and sizing of stationary supercapacitors in a metro network using PSO," in *Proceedings of the IEEE International Conference on Industrial Technology*, 2015, pp. 2680–2685, doi: 10.1109/ICIT.2015.7125493.
- [12] N. Nagaoka *et al.*, "Power compensator using lithium-ion battery for DC railway and its simulation by EMTP," in *IEEE Vehicular Technology Conference*, 2006, pp. 3021–3025, doi: 10.1109/vetecs.2006.1683423.
- [13] W. Kawamura, J. Konno, and A. Sumiya, "1000kW DC/DC Converter Development for DC Traction Stationary BESS Considering Various Operation Power Patterns," in *2022 International Power Electronics Conference, IPEC-Himeji 2022-ECCE Asia*, 2022, pp. 1410–1415, doi: 10.23919/IPEC-Himeji2022-ECCE53331.2022.9807196.
- [14] H. J. Ahmad and M. Hagiwara, "Interleaved Bidirectional Chopper with Auxiliary Converters for DC Electric Railways," *IEEE Transactions on Power Electronics*, vol. 36, no. 5, pp. 5336–5347, 2021, doi: 10.1109/TPEL.2020.3031668.
- [15] K. Tesaki and M. Hagiwara, "Control and Experimental Verification of a Bidirectional Nonisolated DC-DC Converter Based on Switched-Capacitor Converters," *IEEE Transactions on Power Electronics*, vol. 36, no. 6, pp. 6501–6512, 2021, doi: 10.1109/TPEL.2020.3040070.
- [16] P. Bhattacharyya, S. Ghorai, S. Sen, and S. K. Giri, "A Flexible Non-Isolated Multiport Converter to Integrate Battery and Ultracapacitor for Electric Vehicle Applications," *IEEE Transactions on Circuits and Systems II: Express Briefs*, vol. 70, no. 3, pp. 1044–1048, 2023, doi: 10.1109/TCSII.2022.3217844.
- [17] A. Hintz, U. R. Prasanna, and K. Rajashekara, "Novel Modular Multiple-Input Bidirectional DC–DC Power Converter (MIPC) for HEV/FCV Application," *IEEE Transactions on Industrial Electronics*, vol. 62, no. 5, pp. 3163–3172, May 2015, doi: 10.1109/TIE.2014.2371778.
- [18] Y. Dasari, D. Ronanki, and S. S. Williamson, "A Simple Three-Level Switching Architecture to Enhance the Power Delivery Duration of Supercapacitor Banks in Electrified Transportation," *IEEE Transactions on Transportation Electrification*, vol. 6, no. 3, pp. 1003–1012, 2020, doi: 10.1109/TTE.2020.3001024.




- [19] R. Faraji, L. Ding, M. Esteki, N. Mazloum, and S. A. Khajehoddin, "Soft-Switched Single Inductor Single Stage Multiport Bidirectional Power Converter for Hybrid Energy Systems," *IEEE Transactions on Power Electronics*, vol. 36, no. 10, pp. 11298–11315, 2021, doi: 10.1109/TPEL.2021.3074378.
- [20] B. H. Nguyen, T. Vo-Duy, M. C. Ta, and J. P. F. Trovao, "Optimal Energy Management of Hybrid Storage Systems Using an Alternative Approach of Pontryagin's Minimum Principle," *IEEE Transactions on Transportation Electrification*, vol. 7, no. 4, pp. 2224–2237, 2021, doi: 10.1109/TTE.2021.3063072.
- [21] A. Upadhyaya and C. Mahanta, "An Overview of Battery Based Electric Vehicle Technologies With Emphasis on Energy Sources, Their Configuration Topologies and Management Strategies," *IEEE Transactions on Intelligent Transportation Systems*, vol. 25, no. 2, pp. 1087–1111, 2024, doi: 10.1109/TITS.2023.3316191.
- [22] M. R. Larijani, S. H. Kia, M. Zolghadri, A. El Hajjaji, and A. Taghavipour, "Linear Parameter-Varying Model Predictive Control for Intelligent Energy Management in Battery/Supercapacitor Electric Vehicles," *IEEE Access*, vol. 12, pp. 51026–51040, 2024, doi: 10.1109/ACCESS.2024.3385861.
- [23] K. Hadji, K. Hartani, and T. M. Chikouche, "New combined control strategy of on-board bidirectional battery chargers for electric vehicles," *International Journal of Power Electronics and Drive Systems*, vol. 15, no. 1, pp. 303–311, 2024, doi: 10.11591/ijpeds.v15.i1.pp303-311.
- [24] S. Wijanarko, G. I. Hasyim, J. Furqani, A. Rizqiawan, P. A. Dahono, and A. Muqorobin, "A bidirectional power converter connecting electric vehicle battery and DC microgrid," *International Journal of Power Electronics and Drive Systems*, vol. 15, no. 2, pp. 978–992, 2024, doi: 10.11591/ijpeds.v15.i2.pp978-992.
- [25] M. Dhandapani, P. Ravichandran, A. Shanmugam, and N. Pachaivanan, "Performance evaluation of bridgeless isolated SEPIC-Luo converter for EV battery charging using PI and ANN controller," *International Journal of Power Electronics and Drive Systems*, vol. 15, no. 2, pp. 935–946, 2024, doi: 10.11591/ijpeds.v15.i2.pp935-946.
- [26] Z. Li, S. Hoshina, N. Satake, and M. Nogi, "Development of DC/DC converter for battery energy storage supporting railway DC feeder systems," *IEEE Transactions on Industry Applications*, vol. 52, no. 5, pp. 4218–4224, 2016, doi: 10.1109/TIA.2016.2582724.

BIOGRAPHIES OF AUTHORS






Chuen Ling Toh    received the B.Eng. and M.Eng. degree in electrical engineering, both from Universiti Teknologi Malaysia (UTM), Skudai, Malaysia, in 2002 and 2005 respectively; and her Ph.D. in Electrical Power Engineering from Norwegian University of Science and Technology (NTNU), Trondheim, Norway, in 2014. Currently, she is a senior lecturer at the Universiti Tenaga Nasional, Kajang, Malaysia. Her teaching and research interests include the field of power electronics, motor drive systems, and field programmable gate array applications. She is also an engineer registered with Board of Engineers Malaysia and a professional technologist registered with Malaysia Board of Technologists. She can be contacted at email: chuenling@uniten.edu.my.



Ching Sin Tan    received the B.Eng. degree (Hons.) in electrical engineering from Universiti Teknologi Malaysia, in 2000, the M.Sc. and Ph.D. degrees in electrical engineering from the University of Strathclyde, Glasgow, United Kingdom, in 2001 and 2008, respectively. In 2008, he joined Universiti Tenaga Nasional, Malaysia, as a Senior Lecturer. He has involved in various industrial and national projects, particularly in the areas related to energy and climate change. His research interests include power system economics, renewable energy, energy efficiency, and climate change. He is also an engineer registered with Board of Engineers Malaysia and a professional technologist registered with Malaysia Board of Technologists. He can be contacted at email: chingsin@uniten.edu.my.



Chee Wei Tan    received his B.Eng. degree in Electrical Engineering (first class honors) from Universiti Teknologi Malaysia (UTM), in 2003 and a Ph.D. degree in Electrical Engineering from Imperial College London, London, U.K., in 2008. He is currently an associate professor at Universiti Teknologi Malaysia and a member of the Power Electronics and Drives Research Group, Department of Electrical Power Engineering, Faculty of Electrical Engineering. His research interests include the application of power electronics in renewable/alternative energy systems, control of power electronics, and energy management system in microgrids. He is also a Chartered Engineer registered with Engineering Council, UK, a professional engineer registered with Board of Engineers Malaysia and a professional technologist registered with Malaysia Board of Technologists. He is actively participating in IEEE activities and conferences, which he is also the chair of the IEEE Power Electronic Society (PELS) Malaysia Chapter for year 2018. He was awarded the Malaysia Research Star Award (high impact paper—engineering and technologies) 2018 by the Ministry of Education Malaysia. He can be contacted at email: cheewei@utm.my.